

## Head and Neck Cancer Stem Cells: The Side Population

Mark H. Tabor, MD; Matthew R. Clay, BSc; John H. Owen, BSc;  
Carol R. Bradford, MD; Thomas E. Carey, PhD; Gregory T. Wolf, MD; Mark E. Prince, MD

**Objectives/Hypothesis:** The cancer stem cell (CSC) theory concludes that a subpopulation of cancer cells, the cancer stem cells, can self-renew and are responsible for tumor growth. Previous studies have identified cells able to efflux Hoechst 33342 dye as the side population (SP). SP cells and CSCs share many characteristics, suggesting the SP isolated from malignant tumors contains CSCs.

**Study Design:** Experimental Study.

**Methods:** The SP was isolated from a head and neck cancer cell line and analyzed for CSC-like characteristics.

**Results:** The SP demonstrated the ability to reproduce both SP and non-side population (NSP) cells from as few as one cell. The SP had lower expression of active  $\beta$ -catenin and more resistance to 5-fluorouracil; the SP also demonstrated greater expression of Bmi-1 (4.3-fold) and ABCG2 (1.4-fold). SP cells were able to produce tumors in an animal model, whereas NSP were not. SPs were identified in two primary human tumors.

**Conclusions:** This work adds to the evidence that the SP in head and neck cancer represents cells with CSC properties and provides a method by which CSCs can be isolated and studied.

**Key Words:** Head and neck cancer, cancer stem cell, side population, Hoechst 33342, Bmi-1.

**Level of Evidence:** 1c.

*Laryngoscope*, 121:527–533, 2011

### INTRODUCTION

Head and neck cancer is a common malignancy that affects approximately 40,000 new patients in the United States each year.<sup>1</sup> Despite advances in therapy, which have improved quality of life, survival rates have remained static for many years. It is essential that we develop a more complete understanding of the biology of this disease to develop more effective therapies.

A cancer stem cell (CSC) is a cell that possesses the capability to self-renew along with the ability to generate the heterogeneous lineages of cancer cells that comprise the tumor.<sup>2,3</sup> Evidence has been accumulating that supports the validity of the CSC theory in a number of human malignancies.<sup>2,4–11</sup> Recent studies of solid tumors have isolated tumorigenic subpopulations of cancer cells based on their expression of various cell surface

markers. Breast cancer cells that were CD44<sup>+</sup>/CD24<sup>-</sup> and central nervous system cancer cells that expressed CD133 were able to initiate tumors in NOD/SCID mice from as few as 100 cells, as opposed to tens of thousands of cells with different markers.<sup>12–14</sup>

The cell surface marker CD44 was shown to select a tumorigenic subpopulation of cells in head and neck squamous cell carcinoma (HNSCC). As few as  $5 \times 10^3$  CD44<sup>+</sup> tumor cells gave rise to xenograft tumors in NOD/SCID mice, whereas up to  $5 \times 10^5$  CD44<sup>-</sup> tumor cells did not. Tumors resulting from injection of CD44<sup>+</sup> cells reproduced the original tumor heterogeneity, even after serial passages in the animal model, suggesting that the CD44<sup>+</sup> population contains the CSCs.<sup>15</sup>

Goodell et al. reported that a small population of bone marrow cells with an elevated capacity to efflux the vital DNA binding dye Hoechst 33342 could be isolated by flow cytometry. This ability has been attributed to the increased expression of multiple drug resistance transporter proteins such as ABCG2. These cells were termed side population (SP) cells. SP cells have been found to have stem cell-like characteristics, such as a 1,000-fold increase in hematopoietic stem cell (HSC) activity following transplantation into lethally irradiated hosts.<sup>16</sup> SP cells have now been identified in many normal tissues, such as muscle, liver, lung, retina, testes, pancreas, heart, epithelium, and breast, leading many to suggest that the SP phenotype might represent a universal stem cell marker.<sup>17–28</sup>

SP cells isolated from cancer cell lines often have stem cell-like characteristics.<sup>29–35</sup> Chiba et al. found that as few as 1,000 SP cells from a hepatocellular carcinoma cell line could initiate a tumor, as compared to non-SP

From the Department of Otolaryngology–Head and Neck Surgery, University of South Florida, Tampa, Florida (M.H.T.), Department of Molecular and Cell Biology, University of Wisconsin, Madison, Wisconsin (M.R.C.), and the Department of Otolaryngology–Head and Neck Surgery, University of Michigan, Ann Arbor, Michigan, (J.H.O., C.R.B., T.E.C., G.T.W., M.E.P.), U.S.A.

Editor's Note: This Manuscript was accepted for publication April 15, 2010.

This work was supported by the University of Michigan SPORE in Head and Neck Cancer: P50 CA 097248, the Kirschstein National Research Service Award (NRSA) in Advanced Research Training in Otolaryngology: 5 T32 DC005356, and Patricia Korican of Korican Real Estate. The authors have no other funding, financial relationships, or conflicts of interest to disclose.

Send correspondence to Mark E. Prince, MD, Department of Otolaryngology, University of Michigan, Ann Arbor, MI, 48109.  
E-mail: mepp@umich.edu

DOI: 10.1002/lary.21032

(NSP) cells, which had at least 1,000-fold reduced tumorigenicity. Szotec et al. identified a SP in a murine ovarian cancer cell line that was resistant to doxorubicin and in G1 arrest.<sup>35</sup> The SP component of the rat C6 glioma cell line was found to be largely responsible for its *in vivo* malignancy.<sup>29</sup>

Cell lines can provide an essentially unlimited supply of cancer cells, whereas primary cancer cells obtained from patients represent a very limited resource. The ability to identify CSCs in HNSCC cell lines will greatly enhance our ability to study this critical population of cells. The aim of this study was to identify SP cells in an established HNSCC cell line, and determine if these cells had cancer stem cell-like properties.

## MATERIALS AND METHODS

### Cell Culture

UM-SCC-10B is an HNSCC cell line derived from a local recurrence of a true vocal fold cancer that developed one year after radiation therapy. Cells were grown in Dulbecco's Modified Eagle's Medium (DMEM)(Invitrogen, Carlsbad, CA) containing 2 mmol/L L-glutamine, 1% nonessential amino acids, 1% penicillin-streptomycin (Invitrogen), and 10% fetal bovine serum (FBS) in a humidified atmosphere of 5% CO<sub>2</sub> at 37°C.

### Hoechst 33342 Dye Exclusion Assay

Cells were detached from the culture flask with trypsin-ethylenediaminepentaacetic acid (EDTA)(Invitrogen), washed with culture media, and then suspended in DMEM-2% heat-inactivated calf serum (HICS) at a concentration of  $1 \times 10^6$  cells/mL at 37°C. Verapamil hydrochloride (Sigma-Aldrich, St. Louis, MO) was added to control samples at a concentration of 50 mM. Samples were then incubated with Hoechst 33342 (Sigma-Aldrich) at a concentration of 5 µg/mL for 1 hour at 37°C. Following incubation, cells were washed, suspended in Hank's Balanced Salt Solution (HBSS)(Invitrogen) with 2% HICS at  $1 \times 10^6$  cells/mL and kept at 4°C. Propidium iodide (BD Biosciences, San Diego, CA) was added at a concentration of 2 µg/mL to exclude dead cells during flow cytometry. Cells were filtered with a 40-µm cell strainer (BD Biosciences) to ensure a single cell suspension. Cells were analyzed and sorted using the fluorescence-activated cell sorting (FACS) Vantage SE (BD Biosciences). Hoechst 33342 was excited with an ultraviolet laser at 350 nm, and fluorescence emission was measured with DF424/44 (Hoechst blue) and DF630/22 (Hoechst red) optical filters.

### Serum-Free Culture

Cells were cultured in 6-well ultra-low-attachment plates (Corning 3471; Corning Inc., Lowell, MA) at a concentration of 10,000 cells/mL in DMEM/F12 supplemented with B27 (Invitrogen), 20 ng/mL EGF (BD Biosciences), antibiotic-antimycotic (100 unit/mL penicillin G sodium, 100 µg/mL streptomycin sulfate and 0.25 µg/mL amphotericin B)(Invitrogen), 20 µg/mL Gentamycin, 1 ng/mL hydrocortisone, 5 µg/mL insulin and 100 µM 2-mercaptoethanol in a humidified incubator (5% CO<sub>2</sub>, 95% air, 37°C). Spherical clusters of cells were dissociated with trypsin-EDTA (Invitrogen), and washed with HBSS-2% HICS before undergoing the Hoechst dye exclusion protocol described above.

### Chemoresensitivity (3-[4,5-Dimethylthiazol-2-yl]-2,5-Diphenyltetrazolium Bromide) Assay

Following FACS, cells were washed, counted, and plated at 7,000 cells per well in triplicate wells of 96-well plates and incubated in DMEM-10% FBS at 37°C overnight. The next morning, cells were incubated with 5-fluorouracil (5-FU)(Sigma-Aldrich) at increasing concentrations (0, 10, 30, 100, and 1,000 µg/mL) for 2 hours, washed twice with culture media, then incubated in 300 µL DMEM-10% FBS for 6 days. The media was removed from the wells, and 100 µL DMEM along with 10 µL 3-(4,5-dimethylthiazol-2-yl)-2,5-diphenyltetrazolium bromide labeling reagent was added to each well. After a 4-hour incubation, 100 µL of solubilization buffer was added, and the plates were incubated at 37°C overnight. The absorbance of each well was determined with a spectrophotometer at a wavelength of 590 nm. Absorbance at 590 nm is directly proportional to the viable cell number. The absorbance was plotted on a logarithmic graph of absorbance (y-axis) against drug concentration (x-axis). The 50% inhibitory concentrations (IC50) were identified as the concentration of 5-FU required to achieve 50% growth inhibition (i.e., 50% reduction in absorbance relative to no 5-FU control).

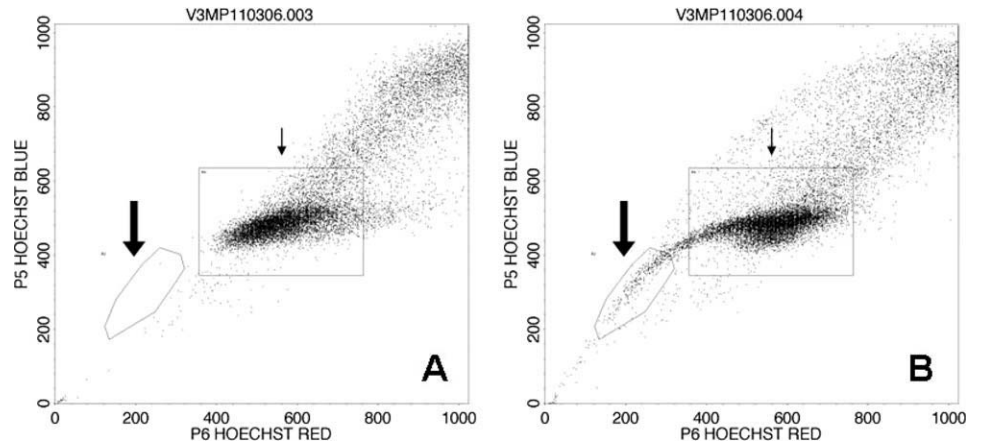
### Quantitative Real-Time Polymerase Chain Reaction

Following FACS, cells were washed twice with phosphate buffered saline (PBS)(GIBCO, Grand Island, NY) before RNA was extracted and purified using the RNeasy Mini kit (Qiagen, Valencia, CA), according to the manufacturer's protocol. The concentration and purity of RNA were determined by a NanoDrop ND-1000 (NanoDrop Technologies, Wilmington, DE) spectrophotometer and Agilent 2100 Bioanalyzer (Agilent Technologies, Palo Alto, CA). cDNA was reverse transcribed with the Promega Reverse Transcription System (Promega, Madison, WI) using random hexamers. The *in vitro* transcription product was purified using the QIAquick PCR Purification Kit (Qiagen) and concentration was determined with the NanoDrop ND-1000 spectrophotometer. Quantitative real-time polymerase chain reaction (PCR) was carried out on an ABI Prism 7900HT Sequence Detection System (Applied Biosystems, Foster City, CA). Primer sets purchased from SuperArray (SuperArray Bioscience Corp., Frederick, MD) included those for the quantification of Bmi-1, ABCG2, and Glyceraldehyde-3-phosphate dehydrogenase (GAPDH)(PPH57778A, PPH01526A and PPH00150A; SuperArray). PCR was performed with 12.5 µL RT<sup>2</sup> Real-Time SYBR Green PCR Master Mix (SuperArray), 1 µL primer set, 1 µL cDNA template, and 10.5 µL H<sub>2</sub>O. Thermocycling was performed as follows: 95°C for 15 minutes, 40 cycles of 95°C for 30 seconds, 55°C for 30 seconds, and 72°C for 30 seconds. Relative quantification (fold difference) of the expression levels of mRNA in each group was calculated by the 2<sup>-ΔΔCT</sup> method.<sup>36</sup> Gene expression data was normalized to GAPDH.

### Immunofluorescence Microscopy

Immediately following FACS, 10,000 cells from each group were suspended in 200 µL DMEM and cytospun onto slides. Cells were fixed in 95% methanol for 15 minutes at -20°C, washed with PBS, and permeabilized with 0.1% triton x-100 in PBS for 5 minutes. Nonspecific binding was blocked with a 30-minute incubation with PBS-1% bovine serum albumin (BSA). Cells were incubated with primary mouse monoclonal antibodies to active-β-catenin (anti-ABC, clone 8E7; Upstate, Lake Placid, NY) or Bmi-1 (anti-Bmi-1, clone F6; Upstate) at 1:200 and 1:300 dilutions in PBS-1% BSA for 1 hour at room

Fig. 1. Flow cytogram of UM-SCC-10B following Hoechst 33342 staining. A: No side population is seen when dye efflux is inhibited with verapamil. B: In the absence of the inhibitor, a side population with low Hoechst 33342 staining is resolved, comprising 2.6% of the cell line (large arrow). The small arrow points to the NSP.



temperature. Cells were washed with PBS and then incubated with goat anti-mouse Alexa Fluor 488 (Invitrogen) secondary antibody at a 1:2000 dilution in PBS-1% BSA for 1 hour at room temperature. Cells were then washed with PBS and incubated with 4',6-diamidino-2-phenylindole at a 1:5000 dilution for 1 minute at room temperature. Coverslips were mounted on slides using ProLong Gold antifade reagent (Invitrogen). Cells were examined and photographed using a Carl Zeiss (Carl Zeiss AG, Oberkochen, Germany) confocal laser scanning microscope.

### Protein Extraction and Western Blot Analysis

Following FACS, protein extracts were prepared by lysing cells in a solution of PBS containing 1% NP-40 (Sigma-Aldrich), 1 mmol/L phenylmethylsulfonyl fluoride (Sigma-Aldrich), and a cocktail of protease inhibitors (Boehringer Ingelheim GmbH, Ingelheim am Rhein, Germany). Total protein from cell extracts was quantified using a colorimetric assay (Bradford Reagent; Bio-Rad, Hercules, CA). For Western blotting, protein (25  $\mu$ g) was electrophoresed on 12% Tris-glycine SDS-polyacrylamide gels under denaturing conditions, and transferred to Hybond-P polyvinylidene difluoride membranes (Amersham Pharmacia Biotech, Buckinghamshire, England). Membranes were blocked in Tris-buffered saline plus 0.05% Tween containing 5% nonfat dry milk at room temperature for 1 hour followed by incubation for 3 hours with primary mouse monoclonal antibodies to active- $\beta$ -catenin (anti-ABC, clone 8E7; Upstate)(1  $\mu$ g/mL), Bmi-1 (anti-Bmi-1, clone F6; Upstate)(1  $\mu$ g/mL) or GAPDH (Chemicon International, Temecula, CA)(1:10,000 dilution). Membranes were then incubated for 1 hour with a secondary horseradish peroxidase-conjugated sheep anti-mouse antibody

(Amersham) and analyzed using the Enhanced Chemiluminescence Plus reagent (Amersham) by exposing membranes to chemiluminescence film (Biomax Light Film; Kodak, Rochester, NY).

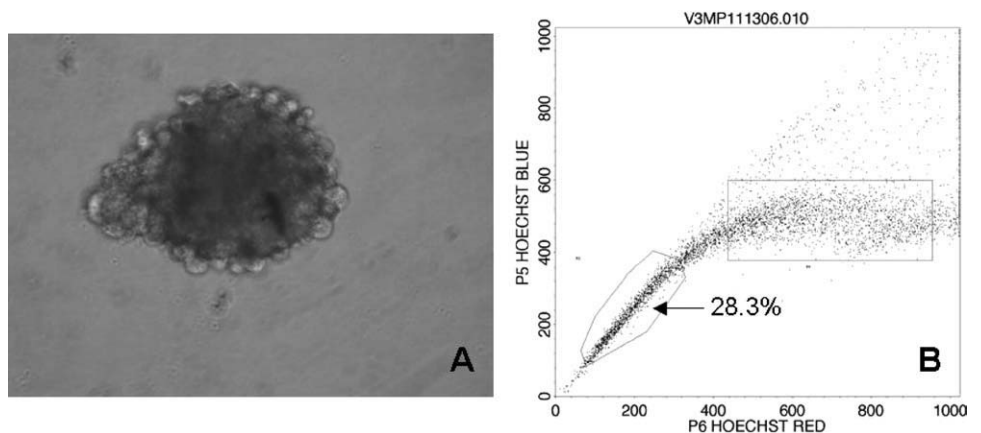
### Primary Tumor Digestion

Approval from the University of Michigan institutional review board was obtained to collect tumor specimens. Informed consent was obtained from patients undergoing surgical resection of their head and neck tumors. Immediately following resection, tumors were cut into small fragments with sterile scissors and minced with a sterile scalpel. The tumor pieces were rinsed with HBSS-2% HICS and centrifuged for 5 minutes at 1,000 rpm. The tissue was placed in a solution of DMEM/F-12 containing 300 U/mL collagenase and 100 U/mL hyaluronidase (Stem Cell Technologies, Vancouver, Canada). The mixture was incubated at 37°C and gently agitated to dissociate the cells. The digestion was arrested with the addition of FBS and cells were filtered through a 40- $\mu$ m cell strainer to allow the passage of only single cells. The cells were washed twice with HBSS-2% HICS and stained for flow cytometry as described above.

### NOD/SCID Mouse Implantations

Approval for the animal experiments was obtained from the University of Michigan University Committee on the Use and Care of Animals. UM-SCC-10B cells were sorted for SP and NSP cells. Five thousand of each cell population, SP and NSP, in single cell suspension were mixed with Matrigel Basement

Fig. 2. Cells formed spheres when grown in serum-free, non-adherent culture (A). The SP increased to 28.3%, a 5.8-fold enrichment when grown in this environment (B).



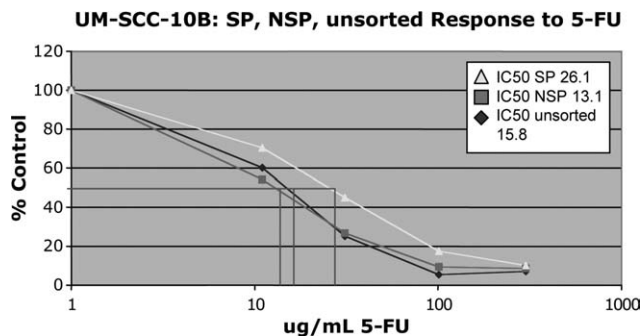


Fig. 3. The SP was more resistant to 5-FU than the NSP or unsorted cells. The SP had an IC<sub>50</sub> of 26.1  $\mu\text{g}/\text{mL}$  which was almost twice that of the NSP, 13.1  $\mu\text{g}/\text{mL}$  or unsorted cells, 15.8  $\mu\text{g}/\text{mL}$ .

Membrane Matrix (BD Pharmingen, San Diego, CA) solution to form a final volume of 200  $\mu\text{L}$ . The cells were then subcutaneously injected into the flank of NOD/SCID mice. Injection sites were sealed with a liquid skin adhesive. The tumorigenicity of the injected cell populations was evaluated by evidence of tumor growth in NOD/SCID mice.

## RESULTS

### Hoechst 33342 Dye Exclusion Assay

An SP in the cell line UM-SCC-10B comprising 2.46%  $\pm$  1.87% of the total cell population was consistently identified. The SP's ability to exclude the dye was inhibited by verapamil hydrochloride, and this was used to differentiate the SP from the NSP (Fig. 1).

### Ability of the SP to Reproduce the Entire Cell Line Phenotype

SP cells were sorted, collected, and transferred to tissue culture flasks. The cells were expanded until approximately  $1 \times 10^6$  cells were obtained. Analysis by flow cytometry demonstrated that the SP was able to reproduce the entire cell line phenotype including both SP and NSP cells. When single SP cells were sorted into 96-well plates and allowed to expand from these clones, they were also found to be capable of reproducing the original cell line heterogeneity.

### Growth in a Serum-Free, Nonadherent Environment

Cells cultured in serum-free media in ultra-low-attachment plates formed multiple spherical colonies. Analysis after Hoechst staining revealed that the SP increased to 28.3%, a 5.8-fold enrichment when compared to an SP of 4.9% in a group of cells growing in a parallel flask in a traditional adherent environment with standard serum-containing media (Fig. 2).

### Chemosensitivity Assay

The SP was more resistant to 5-FU than the NSP or unsorted cells. The SP had an IC<sub>50</sub> of 26.1  $\mu\text{g}/\text{mL}$ , almost twice that of the NSP, 13.1  $\mu\text{g}/\text{mL}$ , or unsorted cells, 15.8  $\mu\text{g}/\text{mL}$  (Fig. 3).

### Protein Expression

Western blot and immunocytochemistry demonstrated that the SP had lower levels of active  $\beta$ -catenin as compared to the NSP (Fig. 4). Immunocytochemistry also showed higher levels of Bmi-1 in the SP as compared to the NSP.

### Gene Expression

The SP expressed higher levels of the genes Bmi-1 and ABCG2 relative to the NSP by real-time quantitative PCR (Fig. 5).

### Identification of Side Populations in Fresh Human Head and Neck Tumors

Tissue was collected from two patients undergoing tumor resection. Following digestion and creation of a single cell suspension, the cells were stained with Hoechst dye and FACS analysis performed. An SP was found in both primary tumors, comprising 0.54% and 0.59% of the total cell population (Fig. 6).

### Tumor Growth in NOD/SCID Mice

The  $5 \times 10^3$  SP cells sorted from UM-SCC-10B produced tumor growth in the animal model in 2/2

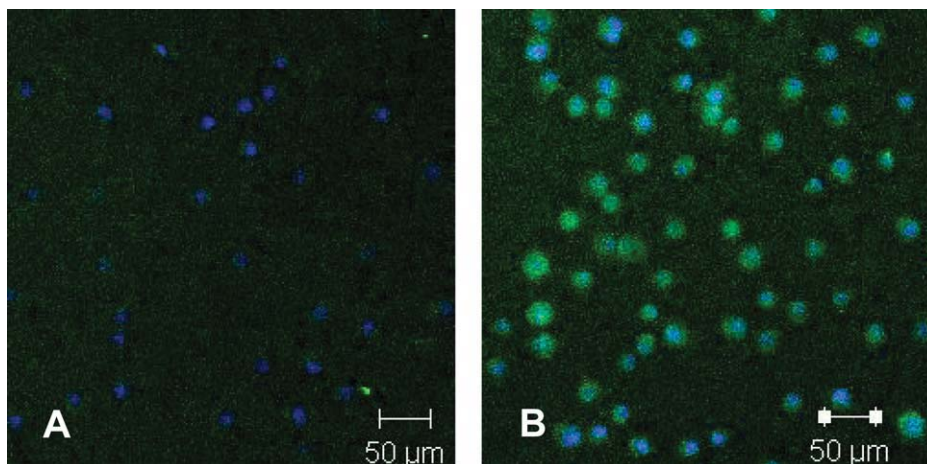


Fig. 4. Immunofluorescence showing that the SP (A) has lower levels of active  $\beta$ -catenin than the NSP (B).

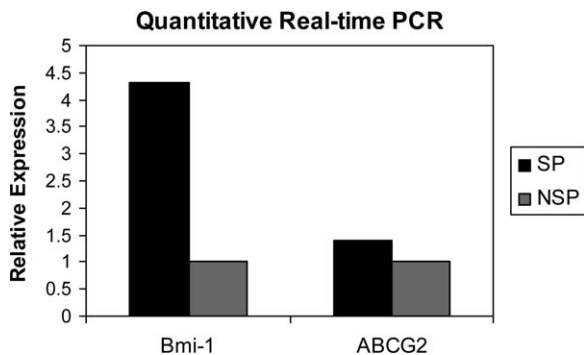


Fig. 5. Relative expression of Bmi-1 (4.32) and ABCG2 (1.41) in the SP compared to NSP.

implantations. The  $5 \times 10^3$  NSP cells did not result in any tumor growth (Table I).

## DISCUSSION

The cancer stem cell theory has important implications for our understanding of cancer biology. Understanding the molecular mechanisms responsible for CSC behavior is crucial to the development of novel treatment strategies. The relatively small size of head and neck tumors, along with the small percentage of CSCs within a tumor, makes CSCs collected from primary tumors a precious and limited experimental resource. An in vitro model for HNSCC CSCs is desperately needed to further study the biology and role of CSCs in this devastating disease. Using the Hoechst 33342 dye exclusion assay we have identified and consistently isolated a small subpopulation of cells from a well-established HNSCC cell line that has stem cell-like properties.

The SP was able to reproduce the entire cancer cell line phenotype from as few as one cell. When expanded and reanalyzed, the SP fraction was enriched but continued to make up only a small population of the entire cell line, suggesting that the SP cell represents a multipotent cell with the potential to undergo asymmetrical cell division. This behavior is consistent with the hierarchical CSC model in which a multipotent cell gives rise to both copies of itself, and to more differentiated progenitors.

Serum-free growth environments have been used to culture neural and mammary stem cells, grown as spheres and termed “neurospheres” or “mammospheres.”<sup>37–42</sup> Epithelial cells are typically dependent upon substrate attachment for survival. The ability to survive in suspension and avoid anoikis and differentiation is thought to be a characteristic of stem cells. Single cell suspensions of UM-SCC-10B in serum-free media in nonadherent plates specifically designed to inhibit attachment resulted in the cells growing in spheres that we termed “squamospheres.” We identified a 5.8-fold increase in the fraction of cells comprising the SP when using this method of culture. We hypothesize that deficiency of serum growth factors and inhibition of attachment encourages the growth of SP cells with their stem cell-like phenotype. This culture method might prove to be an effective way to culture CSCs from primary tumors and cell lines.

The SP was more resistant to the chemotherapeutic agent 5-FU. This is consistent with the CSC phenotype. 5-FU exerts its anticancer effects through inhibition of thymidylate synthase and incorporation of its metabolites into RNA and DNA, inhibiting DNA synthesis and inducing cell death.<sup>43</sup> The drug targets cycling cells that are actively synthesizing DNA, cells that make up the bulk of a tumor. CSCs would be relatively quiescent in comparison to rapidly proliferating progenitor cell and therefore likely to be more resistant to chemotherapeutic agents. Other researchers have shown that stem cells are more resistant to 5-FU. In Zebrafish kidney marrow SP cells exhibiting HSC properties, the SP was found to be more resistant to 5-FU.<sup>44</sup> Wang et al. showed that 5-FU-resistant cancer cell lines had downregulation of cell cycle related genes and delayed passage through S-phase. A greater proportion of 5-FU-resistant cells were found in G<sub>1</sub> or at the G<sub>1</sub>-S boundary and exhibited slower growth rates,<sup>45</sup> as would be expected of stem cells.

$\beta$ -catenin is a central component of the canonical Wnt signaling pathway, wherein Wnt ligands bind to the Frizzled receptor, eventually leading to nuclear

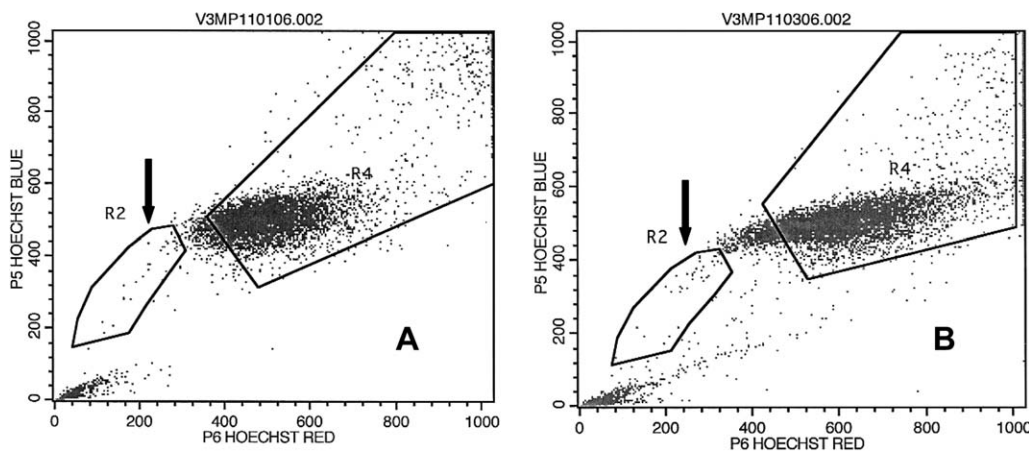


Fig. 6. A SP was identified in two primary head and neck squamous cell carcinoma specimens. The SP (arrows) made up (A) 0.54% and (B) 0.49% of the total cell population.

TABLE I.

Side Population and Non-Side Population Cell Implantations.

Cell Type Implanted	Mouse 1	Mouse 2
SP	Tumor	Tumor
NSP	No growth	No growth

SP = side population; NSP = non-side population.

translocation of active  $\beta$ -catenin and expression of downstream targets. Our results indicate that the SP expresses lower levels of active  $\beta$ -catenin compared to the NSP. This data is consistent with our finding of greater sensitivity of the NSP to 5-FU, where increased nuclear translocation of active  $\beta$ -catenin drives DNA synthesis and cell proliferation, exposing the cell to the toxic effects of a drug such as 5-FU.

Bmi-1 functions as a transcriptional repressor of the senescence-inducing gene  $p16^{\text{Ink4a}}$ , and has been implicated in the self-renewal of stem cells.<sup>46,47</sup> Molofsky et al. were able to show that in the absence of Bmi-1,  $p16^{\text{Ink4a}}$  is upregulated in neural stem cells, reducing their rate of proliferation.<sup>48</sup> Park et al. showed that in Bmi-1-deficient mice, the number of HSCs was markedly reduced.<sup>49</sup> CSCs isolated from HNSCC using CD44 expression were found to overexpress Bmi-1.<sup>15</sup> Our results demonstrated a 4.3-fold increase in Bmi-1 within the SP, lending support to the conclusion that the SP shares cancer stem cell-like properties.

ABCG2 or breast cancer resistance protein-1 is a 70 kDa ATP-binding cassette membrane transport protein, involved in multiple drug resistance by its ability to pump out various drugs. This pump can also actively pump out the DNA-binding dye Hoechst 33342, giving cells with higher expression a lower fluorescence profile and therefore the characteristic SP phenotype.<sup>16</sup> It might be advantageous for a long-lived cell such as a stem cell to have higher expression of ABCG2. Cytotoxic agents could be transported out of the cell before causing DNA damage that would be detrimental to a stem cell, as opposed to a more differentiated cell with limited proliferative potential. We have demonstrated a 1.4-fold increase in expression of ABCG2 in the SP, a characteristic expected of CSCs.

The SP cells were able to induce tumor growth in the animal model, whereas the NSP cells did not. This provides strong evidence that the SP fraction of the cancer cells includes the CSC. We have identified SPs in two primary HNSCC tumor specimens. This suggests that the identification of the SP in head and neck cancer cell lines and primary tumors represents a method by which the CSC subpopulation can be identified for further study.

Currently, there are no well-characterized methods for culturing head and neck CSCs and maintaining them in an undifferentiated state, which seriously limits our ability to study these cells and develop new treatments targeting CSCs. Growth of HNSCC CSCs in serum-free low-attachment conditions might provide a method by which HNSCC CSCs can be efficiently cultured in vitro for study.

## CONCLUSION

SP cells have the defining phenotypical characteristics of CSCs. The Hoechst 33342 dye exclusion assay is a functional assay that provides a simple method by which CSCs can be isolated from HNSCC and supports the growing evidence that it might be a useful method to isolate CSCs in a wide variety of malignant tumors.

## Acknowledgment

The authors would like to acknowledge J. Chad Brenner, MSE, for his technical assistance and intellectual contribution to this work.

## BIBLIOGRAPHY

- Jain S, Khuri FR, Shin DM. Prevention of head and neck cancer: current status and future prospects. *Curr Probl Cancer* 2004;28:265–286.
- Wicha MS, Liu S, Dontu G. Cancer stem cells: an old idea—a paradigm shift. *Cancer Res* 2006;66:1883–1890; discussion 1895–1890.
- Clarke MF, Dick JE, Dirks PB, et al. Cancer stem cells—perspectives on current status and future directions: AACR Workshop on cancer stem cells. *Cancer Res* 2006;66:9339–9344.
- Bonnet D, Dick JE. Human acute myeloid leukemia is organized as a hierarchy that originates from a primitive hematopoietic cell. *Nat Med* 1997;3:730–737.
- Golub TR. Genome-wide views of cancer. *N Engl J Med* 2001;344:601–602.
- Reya T, Morrison SJ, Clarke MF, Weissman IL. Stem cells, cancer, and cancer stem cells. *Nature* 2001;414:105–111.
- Pardal R, Clarke MF, Morrison SJ. Applying the principles of stem-cell biology to cancer. *Nat Rev Cancer* 2003;3:895–902.
- Al-Hajj M, Clarke MF. Self-renewal and solid tumor stem cells. *Oncogene* 2004;23:7274–7282.
- Tai M-H, Chang C-C, Olson LK, Trosko JE. Oct4 expression in adult human stem cells: evidence in support of the stem cell theory of carcinogenesis. *Carcinogenesis* 2005;26:495–502.
- Owens DM, Watt FM. Contribution of stem cells and differentiated cells to epidermal tumours. *Nat Rev Cancer* 2003;3:444–451.
- Li C, Heidt DG, Dalerba P, et al. Identification of pancreatic cancer stem cells. *Cancer Res* 2007;67:1030–1037.
- Al-Hajj M, Wicha MS, Benito-Hernandez A, Morrison SJ, Clarke MF. Prospective identification of tumorigenic breast cancer cells. *Proc Natl Acad Sci U S A* 2003;100:3983–3988.
- Singh SK, Clarke ID, Terasaki M, et al. Identification of a cancer stem cell in human brain tumors. *Cancer Res* 2003;63:5821–5828.
- Singh SK, Hawkins C, Clarke ID, et al. Identification of human brain tumour initiating cells. *Nature* 2004;432:396–401.
- Prince ME, Sivanandan R, Kaczorowski A, et al. Identification of a subpopulation of cells with cancer stem cell properties in head and neck squamous cell carcinoma. *Proc Natl Acad Sci U S A* 2007;104:973–978.
- Goodell MA, Brose K, Paradis G, Conner AS, Mulligan RC. Isolation and functional properties of murine hematopoietic stem cells that are replicating in vivo. *J Exp Med* 1996;183:1797–1806.
- Zhou S, Schuetz JD, Bunting KD, et al. The ABC transporter Bcrp1/ABCG2 is expressed in a wide variety of stem cells and is a molecular determinant of the side-population phenotype. *Nat Med* 2001;7:1028–1034.
- Asakura A, Seale P, Girgis-Gabardo A, Rudnicki MA. Myogenic specification of side population cells in skeletal muscle. *J Cell Biol* 2002;159:123–134.
- Bhattacharya S, Jackson JD, Das AV, et al. Direct identification and enrichment of retinal stem cells/progenitors by Hoechst dye efflux assay. *Invest Ophthalmol Vis Sci* 2003;44:2764–2773.
- Jonker JW, Freeman J, Bolscher E, et al. Contribution of the ABC transporters Bcrp1 and Mdr1a/1b to the side population phenotype in mammary gland and bone marrow of mice. *Stem Cells* 2005;23:1059–1065.
- Lassalle B, Bastos H, Louis JP, et al. “Side population” cells in adult mouse testis express Bcrp1 gene and are enriched in spermatogonia and germinal stem cells. *Development* 2004;131:479–487.
- Summer R, Kotton DN, Sun X, Ma B, Fitzsimmons K, Fine A. Side population cells and Bcrp1 expression in lung. *Am J Physiol Lung Cell Mol Physiol* 2003;285:L97–L104.
- Hussain SZ, Strom SC, Kirby MR, et al. Side population cells derived from adult human liver generate hepatocyte-like cells in vitro. *Dig Dis Sci* 2005;50:1755–1763.
- Shimano K, Satake M, Okaya A, et al. Hepatic oval cells have the side population phenotype defined by expression of ATP-binding cassette transporter ABCG2/BCRP1. *Am J Pathol* 2003;163:3–9.
- Lechner A, Leech CA, Abraham EJ, Nolan AL, Habener JF. Nestin-positive progenitor cells derived from adult human pancreatic islets of Langerhans contain side population (SP) cells defined by expression of the ABCG2 (BCRP1) ATP-binding cassette transporter. *Biochem Biophys Res Commun* 2002;293:670–674.

26. Martin CM, Meeson AP, Robertson SM, et al. Persistent expression of the ATP-binding cassette transporter, *Abcg2*, identifies cardiac SP cells in the developing and adult heart. *Dev Biol* 2004;265:262–275.
27. Oyama T, Nagai T, Wada H, et al. Cardiac side population cells have a potential to migrate and differentiate into cardiomyocytes in vitro and in vivo. *J Cell Biol* 2007;176:329–341.
28. Budak MT, Alpdogan OS, Zhou M, Lavker RM, Akinci MA, Wolosin JM. Ocular surface epithelia contain ABCG2-dependent side population cells exhibiting features associated with stem cells. *J Cell Sci* 2005;118(pt 8): 1715–1724.
29. Kondo T, Setoguchi T, Taga T. Persistence of a small subpopulation of cancer stem-like cells in the C6 glioma cell line. *Proc Natl Acad Sci U S A* 2004;101:781–786.
30. Hirschmann-Jax C, Foster AE, Wulf GG, et al. A distinct “side population” of cells with high drug efflux capacity in human tumor cells. *Proc Natl Acad Sci U S A* 2004;101:14228–14233.
31. Mitsutake N, Iwao A, Nagai K, et al. Characterization of side population in thyroid cancer cell lines: cancer stem-like cells are enriched partly but not exclusively. *Endocrinology* 2007;148:1797–1803.
32. Chiba T, Kita K, Zheng YW, et al. Side population purified from hepatocellular carcinoma cells harbors cancer stem cell-like properties. *Hepatology* 2006;44:240–251.
33. Haraguchi N, Utsunomiya T, Inoue H, et al. Characterization of a side population of cancer cells from human gastrointestinal system. *Stem Cells* 2006;24:506–513.
34. Kruger JA, Kaplan CD, Luo Y, et al. Characterization of stem cell-like cancer cells in immune-competent mice. *Blood* 2006;108:3906–3912.
35. Szotek PP, Pieretti-Vanmarcke R, Masiakos PT, et al. Ovarian cancer side population defines cells with stem cell-like characteristics and Mullerian Inhibiting Substance responsiveness. *Proc Natl Acad Sci U S A* 2006;103: 11154–11159.
36. Livak KJ, Schmittgen TD. Analysis of relative gene expression data using real-time quantitative PCR and the 2(-Delta Delta C(T)) method. *Methods* 2001;25:402–408.
37. Wachs FP, Couillard-Despres S, Engelhardt M, et al. High efficacy of clonal growth and expansion of adult neural stemcells. *Lab Invest* 2003;83: 949–962–.
38. Jensen JB, Parmar M. Strengths and limitations of the neurosphere culture system. *Mol Neurobiol* 2006;34:153–161.
39. Reynolds BA, Tetzlaff W, Weiss S. A multipotent EGF-responsive striatal embryonic progenitor cell produces neurons and astrocytes. *J Neurosci* 1992;12:4565–4574.
40. Reynolds BA, Weiss S. Clonal and population analyses demonstrate that an EGF-responsive mammalian embryonic CNS precursor is a stem cell. *Dev Biol* 1996;175:1–13.
41. Liu S, Dontu G, Mantle ID, et al. Hedgehog signaling and Bmi-1 regulate self-renewal of normal and malignant human mammary stem cells. *Cancer Res* 2006;66:6063–6071.
42. Dontu G, Abdallah WM, Foley JM, et al. In vitro propagation and transcriptional profiling of human mammary stem/progenitor cells. *Genes Dev* 2003;17:1253–1270.
43. Longley DB, Harkin DP, Johnston PG. 5-Fluorouracil: mechanisms of action and clinical strategies. *Nat Rev Cancer* 2003;3:330–338.
44. Tsinkalovsky O, Vik-Mo AO, Ferreira S, Laerum OD, Fjose A. Zebrafish kidney marrow contains ABCG2-dependent side population cells exhibiting hematopoietic stem cell properties. *Differentiation* 2007;75:175–183.
45. Wang W, Cassidy J, O'Brien V, Ryan KM, Collie-Duguid E. Mechanistic and predictive profiling of 5-fluorouracil resistance in human cancer cells. *Cancer Res* 2004;64:8167–8176.
46. Park I-K, Morrison SJ, Clarke MF. Bmi1, stem cells, and senescence regulation. *J Clin Invest* 2004;113:175–179.
47. Valk-Lingbeek ME, Bruggeman SW, van Lohuizen M. Stem cells and cancer; the polycomb connection. *Cell* 2004;118:409–418.
48. Molofsky AV, Pardoll R, Iwashita T, Park I-K, Clarke MF, Morrison SJ. Bmi-1 dependence distinguishes neural stem cell self-renewal from progenitor proliferation. *Nature* 2003;425:962–967.
49. Park IK, Qian D, Kiel M, et al. Bmi-1 is required for maintenance of adult self-renewing haematopoietic stem cells. *Nature* 2003;423:302–305.